Anal. Chem. **2008,** *80,* 2133−2140

Electrochemical Impedance Immunosensor Based on Three-Dimensionally Ordered Macroporous Gold Film

Xiaojun Chen,[†,‡] Yuanyuan Wang,[†] Jinjun Zhou,[†] Wei Yan,[†] Xinghua Li,[†] and Jun-Jie Zhu*[,†]

Key Laboratory of Analytical Chemistry for Life Science, Ministry of Education of China, School of Chemistry and Chemical Engineering, Nanjing University, Nanjing 210093, People's Republic of China, and College of Sciences, Nanjing University of Technology, Nanjing, People's Republic of China

A novel label-free immunosensor for the detection of C-reactive protein (CRP) was developed based on a three-dimensional ordered macroporous (3DOM) gold film modified electrode by using the electrochemical impedance spectroscopy (EIS) technique. The electrode was electrochemically fabricated with an inverted opal template, making the surface area of the 3DOM gold film up to 14.4 times higher than that of a classical bare flat one, characterized by the cyclic voltammetric (CV) technique. The 3DOM gold film which was composed of interconnected gold nanoparticles not only has a good biocompatible microenvironment but also promotes the increase of conductivity and stability. The CRP immunosensor was developed by covalently conjugating CRP antibodies with 3-mercaptopropionic acid (MPA) on the 3DOM gold film electrode. The CRP concentration was measured through the increase of impedance values in the corresponding specific binding of CRP antigen and CRP antibody. The increased electron-transfer resistance (R_{et}) values were proportional to the logarithmic value of CRP concentrations in the range of 0.1 to 20 ng mL^{-1}. The detection of CRP levels in three sera obtained from hospital showed acceptable accuracy.

Since the development of the first glucose biosensor by Clark and Lyons in 1962,[1] electrochemical biosensors have been of high interest due to their rapid and sensitive response as well as the simple and convenient operation. The emergence of nanomaterials has opened new opportunities for electrochemical biosensors.[2] Some particular nanomaterials, such as gold and semiconductor quantum-dot nanoparticles, have already been widely used due to their good biocompatibility.[3,4] Recently, three-dimensional ordered macroporous (3DOM) films have attracted increasing attention due to their fascinating properties, and several methods concerning the synthesis of 3DOM films have been developed.[5−9] Electrodes modified with 3DOM materials can provide large active surface, which is promising to increase functional density and facilitate electron exchange. Xia and co-workers reported the use of a 3DOM gold film modified electrode for the direct electron transfer of hemoglobin[10] and the fabrication of nonenzymatic glucose and methanol sensors.[11,12] Recently, macroporous ultramicroelectrodes (UMEs)[13] and 3DOM Prussian blue (PB) film electrodes[14] have also been prepared for glucose detection. In these systems, the film efficiency or sensing enhancement was significantly higher than that of respective nonporous films.

Due to the highly sensitive and selective nature of the recognition between antigen (Ag) and antibody (Ab), immunoassays are very useful in widespread applications such as medical detection, processing quality control, and environmental monitoring.[15] Traditional methods used in immunoassays involve radioimmunoassay (RIA) and enzyme-linked immunosorbent assay (ELISA). Although they are sensitive, RIA exposes laboratory workers to a significant safety hazard, and ELISA is tedious and time-consuming. New techniques, such as electrochemistry,[16] chemiluminescence,[17] piezoelectricity,[18] and surface plasmon resonance,[19] have attracted extensive interest in immunoassays due to their simple and specific characteristics. Among these techniques, electrochemical immunoassay has received much attention for its high sensitivity and low cost. As most antibodies and antigens are electrochemically inert, the label-free technique of electrochemical impedance spectroscopy (EIS) is developed

* To whom correspondence should be addressed. E-mail: jjzhu@nju.edu.cn.

† Key Laboratory of Analytical Chemistry for Life Science, Ministry of Education of China, School of Chemistry and Chemical Engineering, Nanjing University.

‡ College of Sciences, Nanjing University of Technology.

(1) Clark, L. C.; Lyons, C. *Ann. N.Y. Acad. Sci.* **1962**, *102*, 29−45.
(2) Alivisatos, P. *Nat. Biotechnol.* **2004**, *22*, 47−52.
(3) Rosi, N. L.; Mirkin, C. A. *Chem. Rev.* **2005**, *105*, 1547−1562.
(4) Katz, E.; Willner, I. *Angew. Chem., Int. Ed.* **2004**, *43*, 6042−6108.
(5) Velev, O. D.; Tessier, P. M.; Lenhoff, A. M.; Kaler, W. W. *Nature* **1999**, *401*, 548.
(6) Xu, L.; Zhou, W. L.; Frommen, C.; Baughman, R. H.; Zakhidov, A. A.; Malkinski, L.; Wang, J. Q.; Wiley, J. B. *Chem. Commun.* **2000**, 997−998.
(7) Braun, P. V.; Wiltzius, P. *Adv. Mater.* **2001**, *13*, 482−485.
(8) Braun, P. V.; Wiltzius, P. *Nature* **1999**, *402*, 603−604.
(9) Juárez, B. H.; Golmayo, D.; Postigo, P. A.; López, C. *Adv. Mater.* **2004**, *16*, 1732−1736.
(10) Wang, C. H.; Yang, C.; Song, Y. Y.; Gao, W.; Xia, X. H. *Adv. Funct. Mater.* **2005**, *15*, 1267−1275.
(11) Song, Y. Y.; Zhang, D.; Gao, W.; Xia, X. H. *Chem. Eur. J.* **2005**, *11*, 2177−2182.
(12) Zhang, D.; Gao, W.; Xia, X. H.; Chen, H. Y. *Chin. Sci. Bull.* **2006**, *51*, 19−24.
(13) Szamocki, R.; Velichko, A.; Holzapfel, C.; Mücklich, F.; Ravaine, S.; Garrigue, P.; Sojic, N.; Hempelmann, R.; Kuhn, A. *Anal. Chem.* **2007**, *79*, 533−599.
(14) Qiu, J. D.; Peng, H. Z.; Liang, R. P.; Xiong, M. *Electroanalysis* **2007**, *19*, 1201−1206.
(15) Tang, T. C.; Deng, A.; Huang, H. J. *Anal. Chem.* **2002**, *74*, 2617−2621.
(16) Wilson, M. S. *Anal. Chem.* **2005**, *77*, 1496−1502.
(17) Konry, T.; Novoa, A.; Shemer-Avni, Y.; Hanuka, N.; Cosnier, S.; Lepellec, A.; Marks, R. S. *Anal. Chem.* **2005**, *77*, 1771−1779.
(18) Zuo, B. L.; Li, S. M.; Guo, Z.; Zhang, J. F.; Chen, C. Z. *Anal. Chem.* **2004**, *76*, 3536−3540.
(19) Kurita, R.; Yokota, Y.; Sato, Y.; Mizutani, F.; Niwa, O. *Anal. Chem.* **2006**, *78*, 5525−5531.

10.1021/ac7021376 CCC: $40.75
Published on Web 02/23/2008

to provide a direct detection of immunospecies by measuring the change of impedance. In addition to its convenience, EIS provides a nondestructive means for the characterization of the electrical properties in biological interfaces.[20]

C-reactive protein (CRP) can be synthesized by the liver and is well-known as one of the classical acute-phase reactants and a marker of cardiac and inflammation.[21,22] Generally, the CRP level is less than 2 mg L^{-1} for healthy individuals. However, during an acute phase of inflammation, CRP levels can rapidly increase up to 1000-fold over normal trace amounts, which will make label-free detection an easy task.[23] CRP testing is currently performed with turbidimetric and nephelometric homogeneous immunoassay technologies.[24] However, these methods are not sensitive enough and need expensive clinical analyzers.[25] Therefore, it is important to explore some new routes to detect CRP.

Herein, a highly sensitive label-free immunosensor for the detection of CRP was developed, based on EIS and a 3DOM gold film modified electrode. The electrode was electrochemically synthesized by an inverted opal template and characterized by cyclic voltammetry (CV), scanning electron microscopy (SEM), and X-ray diffraction (XRD). The 3DOM gold film was first covalently assembled with 3-mercaptopropionic acid (MPA), and then CRP antibodies were combined to the MPA-modified electrode to yield the sensing interface. After that, the unreacted covalent-active surface groups were passivated by bovine serum albumin (BSA). The resulting 3DOM-modified electrode was tested as an EIS immunosensor for CRP detection. To the best of our knowledge, we have not found reports about the EIS immunosensor based on a 3DOM gold film electrode. This method is cost-effective, versatile, and highly sensitive for immunoassays. The detailed optimization and attractive performance characteristics of the developed immunosensor are reported in the following sections.

EXPERIMENTAL SECTION

Chemicals and Materials. CRP-Ag (10.2 mg dL^{-1}) and polyclonal affinity-purified CRP-Ab (4.89 mg mL^{-1}) were gifts from the Pointe Biotech. Co. Ltd. Human serum samples were obtained from Nanjing Gulou Hospital and used as received. *N*-Hydroxysuccinimide (NHS) and 3-mercaptopropionic acid (MPA) were purchased from Aldrich (St. Louis, MO). Bovine serum albumin (BSA, 96−99%) was obtained from Sigma (St. Louis, MO). 1-Ethyl-3-(3-dimethylaminopropyl) carbodiimide hydrochloride (EDC) was purchased from Pierce (Rockford, IL). Phosphate-buffered saline (PBS buffer, 10 mM, pH 7.4) were prepared by varying the ratio of NaH_2PO_4 and Na_2HPO_4. The standard CRP-Ag solutions were prepared daily in the PBS buffer solution, and the CRP-Ab was stored at 4 °C. All other chemicals, such as tetraethoxysilane (TEOS, 98%), anhydrous ethanol (EtOH), acetone, H_2SO_4, H_2O_2, NaOH, and $HAuCl_4 \cdot 4H_2O$, $NH_3 \cdot H_2O$ (25%) were of analytical grade. Ultrapure fresh water obtained from a Millipore water purification system (MilliQ, specific resistivity >18 MΩ cm, S.A., Molsheim, France) was used in all runs.

Apparatus. All electrochemical experiments were carried out on a CHI660B electrochemical workstation (Shanghai CH Instruments Co.) using a traditional three-electrode system. A platinum foil and a saturated calomel electrode (SCE) were used as counter electrode and reference electrode, respectively, and the 3DOM gold film modified electrode was used as working electrode. All potentials herein are referenced to the SCE. The geometric area of the working electrode was controlled by insulating tape covering the edges of SiO_2 layers and determined to be 0.07 cm^2. The size of the prepared monodispersed SiO_2 spheres was determined from transmission electron microscopy (TEM, JEOLJEM-200CX) and a Brookhaven BI-9000AT laser dynamic light scattering (DLS) system (Brookhaven Instruments Corporation, U.S.A.). The morphology of the 3DOM gold films was verified by SEM (Philips XL30 series ESEM, using an accelerating voltage of 20 kV) and a Philip-X'Pert X-ray diffractometer taken with a Cu Kα X-ray source.

Preparation of Monodisperse Silica Spheres. Monodisperse SiO_2 spheres with diameter of ∼500 nm (relative standard deviations 3.8%) were synthesized by using a sonochemical technique varied from the Stöber method.[26] Three solutions were prepared in the experiments: solution A was composed of 0.44 mL of TEOS and 11.2 mL of EtOH, solution B included 2.82 mL of ammonia and 11.2 mL of EtOH, and solution C was composed of 2.2 mL of TEOS and 22.2 mL of EtOH. First, solutions A and B were mixed quickly under ultrasonic stirring at 25 °C for 10 min. Then 2.78 mL of ammonia was added. After 5 min, solution C was introduced into the system. A volume of 2.78 mL of ammonia was successively added every 5 min, then, solution C was added again after another 5 min. The addition process repeated five times. Finally, the total system was left for 2 h after being stirred for 5 min. The as-synthesized silica alcosol was washed with anhydrous EtOH by six centrifugation/dispersion cycles in order to remove impurities, such as ammonia, water, and unreacted TEOS. After characterizations, these particles were sintered at 200 °C for 2 h, and then redispersed in EtOH.

Preparation of 3DOM Gold Films. Gold substrates were provided by the 55th Institute of China Electronic Group (Nanjing, China). They were prepared by sputtering a 200 nm thick gold top layer onto the quartz wafers, which was previously coated with a few nanometers of Cr adhesion layer under vacuum. Before use, gold substrates were cleaned with acetone in an ultrasonic bath for 10 min and dried under nitrogen flow, followed by immersion in a piranha solution (7:3 v/v, H_2SO_4/H_2O_2) for 1 min in order to get rid of inorganic and organic contaminants on the substrate surface. The gold substrates were subsequently rinsed thoroughly with absolute EtOH and finally dried under nitrogen flow. Scheme 1 shows the fabrication procedure of the preparation of the 3DOM gold electrode. First, the vertical deposition technique was used to assemble the silica spheres on the gold substrates, forming (111) close-packed crystals (Scheme 1b). Before metal was deposited, the silica colloidal crystals were sintered at 200 °C under nitrogen atmosphere for 2 h. This sintering step ensured the mechanical strength of the template and the formation of small necks between neighboring spheres. Those small necks were

(20) Chen, H.; Jiang, J. H.; Huang, Y.; Deng, T.; Li, J. S.; Shen, G. L.; Yu, R. Q. *Sens. Actuators, B* **2006**, *117*, 211−218.
(21) Whicher, J.; Biasucci, L.; Rifai, N. *Clin. Chem. Lab. Med.* **1999**, *37*, 495−503.
(22) Pentikanen, M. O.; Oorni, K.; Ala-Korpela, M.; Kovanen, P. T. *J. Intern. Med.* **2000**, *247*, 359−370.
(23) Vikholm-Lundin, I. *Biosens. Bioelectron.* **2006**, *21*, 1141−1148.
(24) Roberts, W. L.; Moulton, L.; Law, T. C.; Farrow, G.; Cooper-Anderson, M.; Savory, J.; Rifai, N. *Clin. Chem.* **2001**, *47*, 418−425.
(25) Husebekk, A.; Hansson, L. O. In *C-reactive Protein in Clinical Practice*; Nycomed Pharma AS: Oslo, Norway, 1999; pp 1−49.
(26) Stöber, W.; Fink, A.; Bohn, E. *J. Colloid Interface Sci.* **1968**, *26*, 62−69.

Scheme 1. Procedure for Preparation of 3DOM Gold Film Electrodes

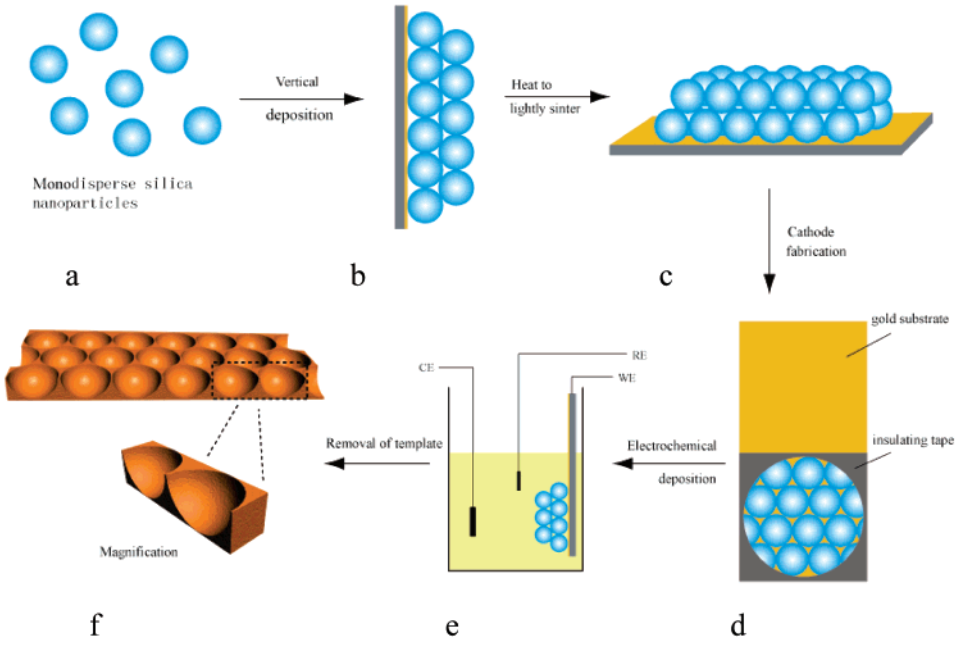

Scheme 2. Schematic Illustration of the Stepwise Immunosensor Fabrication Process

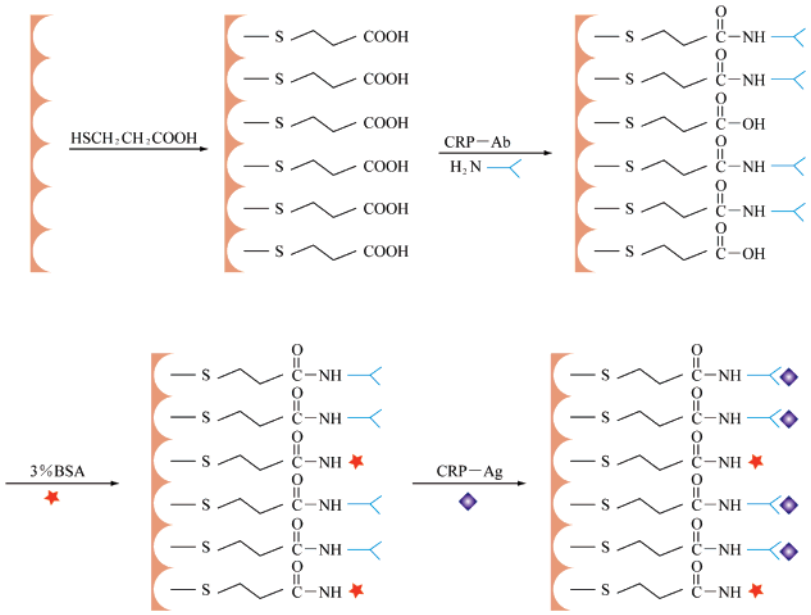

essential for the following etching off the silica colloid template steps and create interconnections among the pores (Scheme 1c). The electrode area was controlled by an apertured insulating tape covering the edge of SiO_2 layers and was determined to be 0.07 cm^2 (Scheme 1d). Then, it was immersed into a mixture of 0.1% (w/w) $HAuCl_4$ and 0.1 M $HClO_4$ solution for 1 h prior to electrolysis. Gold was then electrodeposited into the interspaces of the silica-crystal template at a potential of 0.5 V. To ensure that the electrons could only be used to reduce Au^{III} ions, the electrolyte solution was deaerated with N_2 and N_2 flowed over the solution throughout the whole process (Scheme 1e). After electrodeposition, an ordered through-pore array was formed by dissolving the template in aqueous HF (5%) for about 5 min. The magnification shows that the 3DOM gold film was actually composed of interconnected nanoparticles (Scheme 1f).

Fabrication of the Immunosensor. After the preparation of the 3DOM gold film electrode, it was electrochemically cleaned by cyclic scanning with a potential range of 0 to 1.5 V in 0.1 M H_2SO_4 at a scan rate of 100 mV s^{-1}. The 3DOM gold electrode was first dipped in 2 mM MPA aqueous solution for 24 h at 4 °C. After thoroughly rinsed with ultrapure water to remove physically adsorbed MPA, it was immersed in a solution with 20 mg mL^{-1} of EDC and 10 mg mL^{-1} of NHS for 1 h. After the activated 3DOM gold film/MPA was thoroughly rinsed with PBS, it was soaked in 489 μg mL^{-1} of CRP-Ab PBS solution overnight to yield sensing interfaces. Then, unbound antibodies were washed away with PBS.

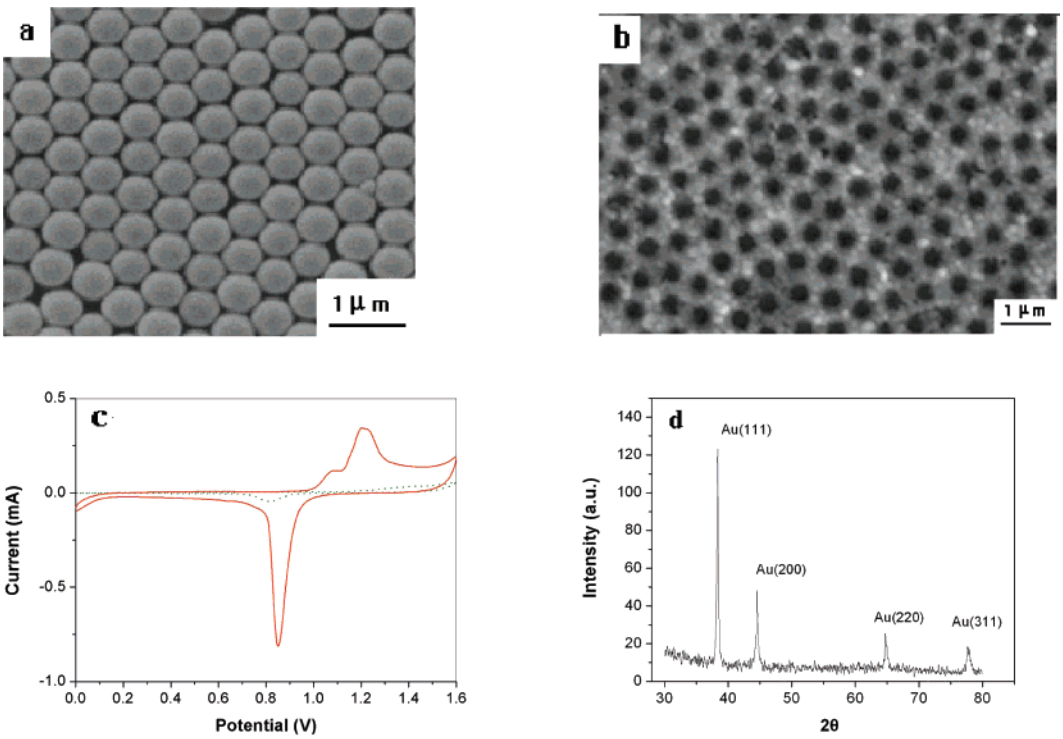

Figure 1. (a) SEM image of the silica template. (b) SEM image of the 3DOM gold film after removal of the silica template. (c) Cyclic voltammograms of the macroporous gold film electrode in 0.1 M H_2SO_4 at a scan rate of 100 mV s^{-1} (solid curve). For comparison, the CV of a flat gold electrode is also shown (dotted curve). (d) X-ray diffraction pattern of the macroporous gold film.

The unreacted covalent-active surface groups were subsequently passivated by reaction with 3% (w/w) BSA at room temperature for 3 h, followed by washing carefully 3 times with PBS. The fabricated CRP immunosensor was stored at 4 °C when not in use. The fabrication process is shown in Scheme 2.

Electrochemical Measurements. The prepared CRP immunosensor was incubated in 0.5 mL of incubation solution containing different concentrations of CRP-Ag at 37 °C for 60 min and washed carefully with PBS. The electrochemical measurements including CV and EIS were performed in a degassed PBS solution containing 0.1 M KCl and 2 mM $Fe(CN)_6^{3-}$/$Fe(CN)_6^{4-}$.

The real serum samples were diluted to the appropriate concentrations (1 to 10 ng mL^{-1}) with PBS buffer, respectively. The data of condition, optimization, and calibration curve were the average of three measurements.

RESULTS AND DISCUSSION

Preparation of the Macroporous Gold Film Electrode. Monodispersed SiO_2 spheres were first assembled on gold slides to form a highly ordered colloidal crystal template using the vertical deposition technique. The SEM image showed that the silica template consisted of close-packed silica spheres with diameter of ~500 nm (Figure 1a). In comparison with the traditional Stöber method, the ultrasonic-assisted preparation used here is much more facile and time-saving. Gold was then electrochemically deposited into the interspaces of the silica-crystal template at a potential of 0.5 V. The amount of gold deposited in the template can be determined and controlled by the charge passed through the cell. After chemical removal of the silica template with aqueous HF, a highly ordered macroporous gold film was obtained. As shown in Figure 1b (0.1 C charge was passed during electrodeposition), the electrodeposited gold film consists of an interconnected, periodic hexagonal array of monodispersed pores. The gold film was electrochemically characterized in 0.1 M H_2SO_4 at a scan rate of 100 mV s^{-1} as shown in Figure 1c, solid curve. For comparison, the voltammogram of a bare flat gold electrode with the same geometric surface area is also presented in Figure 1c, dotted curve. Gold oxidation started at about 1.0 V, showing two anodic current peaks. The formed gold oxide was then electrochemically reduced in the negative potential sweep. By integrating the charge required for reducing the gold oxide formed in the positive sweep, the real surface area of the gold film electrode was determined to be 1.01 cm^2. Assuming that the reduction of a monolayer of gold oxide requires 386 μC cm^{-2},[27] whereas the geometrical area of the bare flat gold electrode was only 0.07 cm^2, the roughness factor (R_f) of the 3DOM gold film was calculated to be 14.4. Obviously, the interconnected, three-dimensionally ordered gold film electrode has a much larger area than the real surface, in addition to a microenvironment conductive to the efficient alignment of protein molecules due to the biocompatible affinity of Au in the 3DOM structure. Figure 1d shows the XRD patterns of the 3DOM gold film. The position and intensity of the four diffraction peaks match well with (111), (200), (220), (311) crystal faces of cubic phase Au (JCPDF04-0784). The diffraction peaks are broadening, which indicates that the gold product is composed of small particles with average size of 32.2 nm calculated by the Debye−Scherrer equation.

(27) Kozlowska, H. A.; Conway, B. E.; Hamelin, A.; Stoicoviciu, L. *J. Electroanal. Chem.* **1987**, *278*, 429−453.

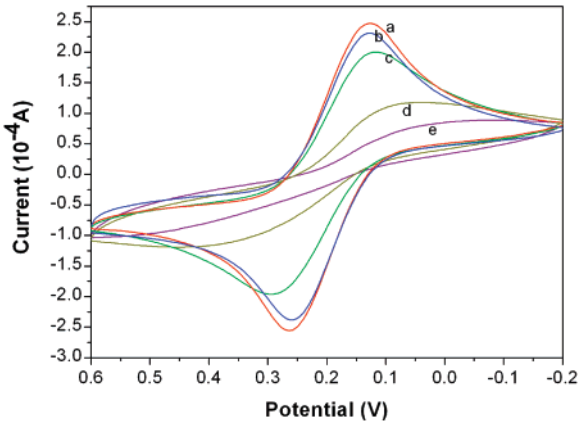

Figure 2. Cyclic voltammograms of a modified 3DOM gold electrode recorded in PBS (10 mM, pH 7.4) solution containing 0.1 M KCl and 2 mM $Fe(CN)_6^{3-}/Fe(CN)_6^{4-}$: (a) 3DOM gold electrode; (b) MPA/3DOM gold electrode; (c) CRP-Ab/MPA/3DOM gold electrode; (d) BSA/CRP-Ab/MPA/3DOM gold electrode; (e) CRP-Ag/BSA/CRP-Ab/MPA/3DOM gold electrode. The scan rate was 100 mV s^{-1}.

Electrochemical Characteristics of the Electrode Surface. All electrochemical measurements were performed in PBS solution containing 0.1 M KCl and 2 mM $Fe(CN)_6^{3-}/Fe(CN)_6^{4-}$. The CV of ferricyanide was chosen as a marker to investigate the changes of the electrode behavior after each assembly step. Figure 2 shows the CV of $Fe(CN)_6^{3-/4-}$ at the 3DOM gold electrode (curve a), MPA-combined electrode (curve b), CRP-Ab-modified electrode (curve c), CRP-Ab-modified electrode blocked with BSA (curve d), and CRP antigen combined electrode (curve e), respectively. As shown in Figure 2, stepwise modification on the 3DOM gold electrode was accompanied by a decrease in the amperometric response and an increase in the peak-to-peak separation between the cathodic and anodic waves of the redox probe, showing that the electron-transfer kinetics of $Fe(CN)_6^{3-/4-}$ is obstructed. After the 3DOM gold film electrode was functionalized with MPA, the electron transfer between the electrochemical probe and electrode surface was inhibited, owing to the electrostatic repulsion of MPA with negative charges and the negatively charged electrochemical probe. When CRP-Ab and BSA were immobilized on the electrode surface, the peak currents of the redox couple of $Fe(CN)_6^{3-}/Fe(CN)_6^{4-}$ decreased again. In particular, after CRP antigen molecules were combined with the antibody molecules, an obvious disappearance of the anodic peak and cathodic peak was observed (curve e).

EIS can also give detailed information on the impedance changes in the modification process. The impedance spectra include a semicircle portion and a linear portion. The semicircle portion at higher frequencies corresponds to the electron-transfer-limited process, and the linear portion at lower frequencies represents the diffusion-limited process. The semicircle diameter equals the electron-transfer resistance, R_{et}. Figure 3A shows the Faradaic impedance spectra observed upon the stepwise modification process. The 3DOM gold film modified electrode reveals a very small semicircle domain (curve a), implying a very low electron-transfer resistance of the redox probe. After the electrode was conjugated with MPA, the R_{et} was slightly bigger (curve b), showing that the self-assembled layers of COO^- terminal groups on the electrode surface generated a negatively charged surface that reduced the ability of the redox probe to access the layer.[28]

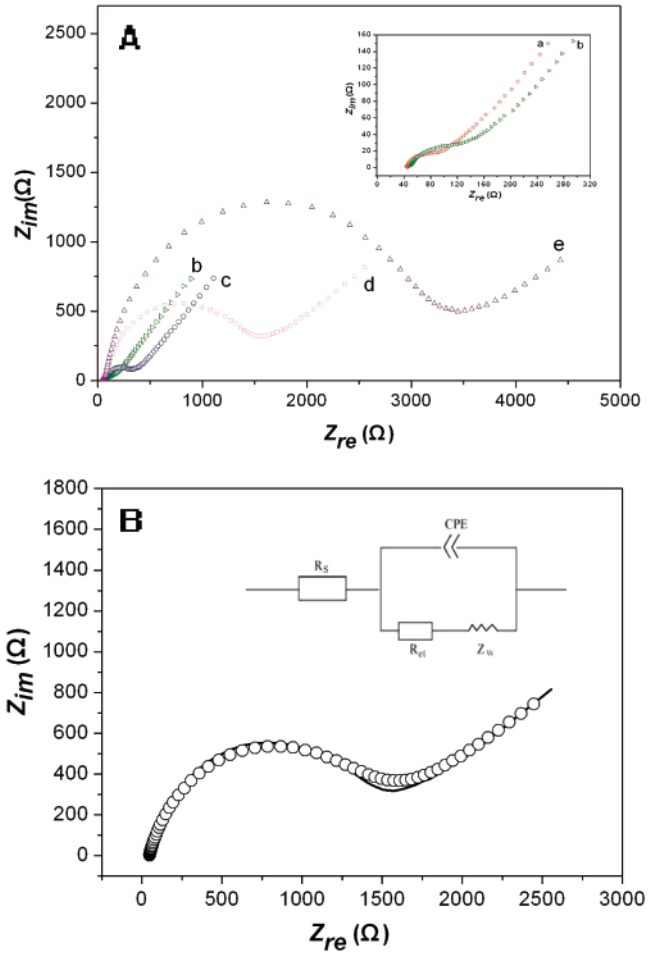

Figure 3. (A) Nyquist plots of a modified 3DOM gold electrode recorded in PBS (10 mM, pH 7.4) solution containing 0.1 M KCl and 2 mM $Fe(CN)_6^{3-}/Fe(CN)_6^{4-}$: (a) 3DOM gold electrode; (b) MPA/3DOM gold electrode; (c) CRP-Ab/MPA/3DOM gold electrode; (d) BSA/CRP-Ab/MPA/3DOM gold electrode; (e) CRP-Ag/BSA/CRP-Ab/MPA/3DOM gold electrode. The frequency range is from 0.01 Hz to 100 kHz with a signal amplitude of 5 mV, and the scan rate was 100 mV s^{-1}. The inset is the plots of (a) and (b). (B) Fitted (solid line) and experimental (scattered line) Nyquist plots of impedance spectra. The inset is the equivalent circuit applied to fit the impedance spectroscopy using a constant phase element (CPE) instead of capacitance owing to the rough surface in the presence of the redox couple of $Fe(CN)_6^{3-/4-}$.

Subsequently, CRP antibodies were covalently combined on the MPA-modified electrode and the R_{et} increased again (curve c), after the electrode was blocked with BSA, the R_{et} increased greatly (curve d), and R_{et} increased in the same way when the immunosensor was used to detect the CRP-Ag (curve e). The reason is that the protein layer on the electrode acted as the inert electron and mass-transfer blocking layer, and they hindered the diffusion of ferricyanide toward the electrode surface significantly. Additionally, since the isoelectric points (pI) of CRP-Ab, CRP, and BSA are 7.6, 5.1, and 4.7, respectively,[29,30] at pH 7.4, CRP and BSA are negatively charged, whereas CRP-Ab is positively charged,

(28) Li, Z. P.; Liu, C. H.; Su, Y. Q.; Duan, X. R. *Chem. J. Internet* [Online] **2005**, *7*, 83. http://www.chemistrymag.org.
(29) Pei, R.; Cheng, Z.; Wang, E.; Yang, X. *Biosens. Bioelectron.* **2001**, *16*, 355–361.
(30) Laurent, P.; Potempa, L. A.; Gewurz, G.; Fiedel, B.A.; Allen, A. C. *Electrophoresis* **2005**, *4*, 316–317.

so BSA and CRP could block the electron transmission transfer much more severely than CRP-Ab. In the modification process, it was obvious that the impedance values of curves d and e were much larger than those of previous reports,[31−34] indicating that the 3DOM gold film could greatly enhance the amount of immobilized proteins because of its larger active surface area. The results were consistent with the CV curves shown in Figure 2. In comparison with CV, the results of EIS presented more apparent differences to multilayers deposited on the 3DOM gold film electrode, indicating better sensitivity.

The impedance data were fitted with commercial software Zview2. A modified Randle's equivalent circuit and the fitting of one measured spectrum to the equivalent circuit (solid line) are both shown in Figure 3B, indicating good agreement with the circuit model and the measurement system over the entire measurement frequency range. The circuit, which is often used to model interfacial phenomena, includes the following four elements: (i) the ohmic resistance of the electrolyte solution, R_s; (ii) the Warburg impedance, Z_w, resulting from the diffusion of ions from the bulk electrolyte to the electrode interface; (iii) the interfacial double layer capacitance (C_{dl}) between an electrode and a solution, relating to the surface condition of the electrode; since the surface of the 3DOM gold film electrode was very rough, it had a larger real surface area; therefore, we used a constant phase element (CPE) instead of the classical capacitance to fit the impedance data, because the electrolyte side of the interface dominated the impedance of the interface;[35−37] (iv) the electron-transfer resistance, R_{et}, which exists if a redox probe is present in the electrolyte solution. The parallel elements (CPE and Z_w + R_{et}) of the equivalent circuit were introduced since the total current through the working interface was the sum of respective contributions from the Faradaic process and the double layer charging. Ideally, Z_w and R_s represented the bulk properties of the electrolyte solution and diffusion features of the redox probe in solution and, thus, are not affected by modifications on the electrode surface. A negligible change in R_s was observed during the modification process. As shown in Figure 3A, further results demonstrate that the ohmic resistance of the solution was not affected by the modification of electrode. At the same time, as can also be seen in Figure 3A, the changes in R_{et} were much larger than those in other impedance components. Thus, R_{et} was a suitable signal for sensing the interfacial properties of the prepared immunosensor during all these assembly procedures.

Detection of CRP Antigen. The fitting values for the stepwise assembled layers on the electrode are presented in Table 1. For the macroporous gold film electrode, the value of R_{et} is 68 Ω, exhibiting a nearly straight line in the Nyquist plot of impedance spectroscopy (Figure 3A, curve a), showing a diffusion-limited electron-transfer process. After the assembly of MPA, the value of R_{et} was 152 Ω (Figure 3A, curve b), slightly bigger than that of the bare macroporous electrode. After immobilization of CRP antibody, an obvious semicircle part of the impedance spectrum was observed, and R_{et} increased to 368 Ω (Figure 3A, curve c). A remarkable increase in R_{et} to 1498 Ω (Figure 3A, curve d) was shown in the successive step of BSA obturation. The increase of R_{et} value was associated with the blocking behavior of the assembled layer on the electrode surface for the redox probe $Fe(CN)_6^{3-/4-}$, reflecting in the impedance spectroscopy as the increase in the diameter of the semicircle at high frequencies. These results were consistent with those obtained by CV measurements. After the immobilization of CRP-Ag on the electrode, R_{et} became very high, 3354 Ω (Figure 3A, curve e). The reason was that CRP antibody, antigen, and BSA are all insulated, and they hindered the diffusion of the electrochemical probe toward the electrode surface.

Table 1. Electrochemical Impedance Results for Stepwise Assembled Electrodes Obtained from Figure 3

electrode	R_{et}(Ω)
bare gold film electrode (Au film)	68
MPA/Au film	152
Ab/MPA/Au film	368
BSA/Ab/MPA/Au film	1498
Ag/BSA/Ab/MPA/Au film	3354

To evaluate the reaction between Ab and Ag, we exposed the BSA/Ab/MPA/Au film electrode to various concentrations of CRP antigen C_{Ag}. The corresponding Nyquist plots of impedance spectra are shown in Figure 4A, and the fitting values of R_{et} are presented in Table 2. It was found that the diameter of the Nyquist circle increased with the adding of antigen. This may be because more antigen molecules bind to the immobilized antibodies in higher concentrations of antigens, which acts as a definite kinetic barrier for the electron transfer. The electrochemical CRP immunosensor displayed well-defined concentration dependence. As shown in Figure 4B, a linear relation between the relative R_{et} responses and the logarithmic value of antigen concentrations was observed in a range from 0.1 to 20.0 ng mL^{-1}. The linear regression equation is $\Delta R_{et}(\Omega) = 4215.8 + 2651.7 \log C_{Ag}$ (ng mL^{-1}) with a correlation coefficient 0.992 ($n = 6$). The lowest detection limit of CRP antigen concentration was 0.1 ng mL^{-1}. According to the linear equation, we could detect CRP concentration quantitatively. Higher serum CRP levels could be detected by an appropriate dilution with pH 7.4 PBS.

In Table 2, the change in R_{et} (ΔR_{et}) is calculated by the following equation:

$$\Delta R_{et} = R_{et(Ag-Ab)} - R_{et(BSA)} \quad (1)$$

where $R_{et(Ag-Ab)}$ is the value of the electron-transfer resistance after CRP-Ag coupling to the immobilized Ab on the gold film electrode. $R_{et(BSA)}$ represents the value of the impedance after blocking the remaining adsorption-reactive sites by BSA. As can be seen, ΔR_{et} increased with increasing antigen concentrations within the detection range. However, the increases in ΔR_{et} were not obvious at higher antigen concentrations due to steric hindrance or saturation of coupled antigen molecules.

Optimization of Experimental Conditions. The combination of proteins on the 3DOM gold film electrode could change the

(31) Yuan, R.; Tang, D.; Chai, Y.; Zhong, X.; Liu, Y.; Dai, J. *Langmuir* **2004**, *20*, 7240−7245.
(32) Huang, H. Z.; Liu, Z. G.; Yang, X. R. *Anal. Biochem.* **2006**, *356*, 208−214.
(33) Dong, H.; Li, C. M.; Chen, W.; Zhou, Q.; Zeng, Z. X.; Luong, J. H. T. *Anal. Chem.* **2006**, *78*, 7424−7431.
(34) Yang, L.; Li, Y.; Erf, G. F. *Anal. Chem.* **2004**, *76*, 1107−1113.
(35) Pajkossy, T. J. *Electroanal. Chem.* **1994**, *364*, 111−124.
(36) De Levie, R. *Electrochim. Acta* **1965**, *10*, 113−130.
(37) Scheider, W. *J. Phys. Chem.* **1975**, *79*, 127−136.

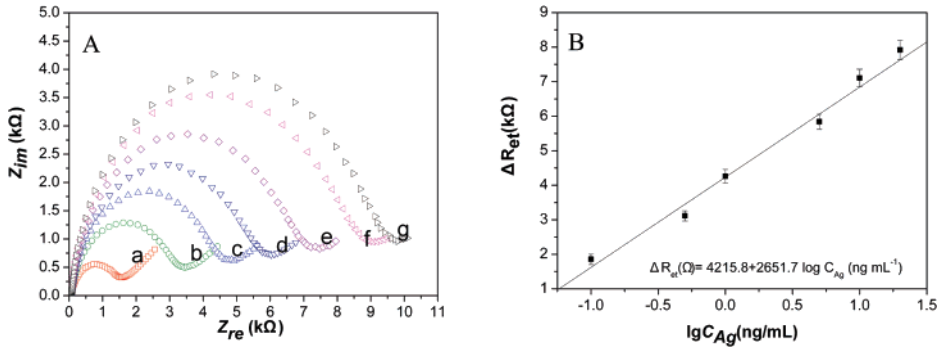

Figure 4. (A) Faradaic impendence spectra that corresponded to the 3DOM gold electrode before and after incubating with different concentrations of CRP antigen in PBS (10 mM, pH 7.4) solution containing 0.1 M KCl and 2 mM $Fe(CN)_6^{3-/4-}$: (a) blank solution; curves b−g represent 0.1, 0.5, 1.0, 5.0, 10.0, and 20.0 ng mL^{-1} CRP antigen, respectively. (B) Calibration curve for the CRP immunosensor.

Table 2. Electrochemical Impedance Results for Antigen−Antibody Interaction from Figure 4A

concn of antigen (ng/mL)	$R_{et}(\Omega)$	$\Delta R_{et}(\Omega)$
0.1	3354	1856
0.5	4612	3114
1.0	5760	4262
5.0	7039	5541
10.0	8603	7105
20.0	9419	7921

interface properties of electrodes, resulting in a change of R_{et}. Several factors, such as Ag incubation temperature and incubation time, were investigated.

The effect of incubation temperature on the EIS value for the antibody−antigen reaction was studied in a temperature range of 20−50 °C. The CRP-Ab and BSA modified 3DOM gold film electrode was immersed in 0.1 ng/mL CRP-Ag solution at different temperatures for 60 min. The electron-transfer resistance, R_{et}, was recorded by Faradic impedance measurement. The maximum response occurred at a reaction temperature of 37 °C, as shown in Figure 5A.

Adsorption time also greatly affected the Ag−Ab combination. The CRP-Ab and BSA modified 3DOM gold film electrode was immersed in 0.1 ng/mL CRP-Ag solution at 37 °C for different time periods. The effect of reaction time on the EIS response is shown in Figure 5B. With the increase of reaction time, the electrochemical response of the immunological reaction increased and then reached a plateau when the reaction time was longer than 60 min.

As a result, an incubation temperature of 37 °C and reaction time of 60 min were selected for the immunoassay of CRP antigen combining the immobilized antibody.

Nonspecific Interactions. Usually, nonspecific adsorption is a major problem in label-free immunosensing, since it cannot be distinguished from specific adsorption in unlabeled electrochemical sensing antigens. To confirm that the above-observed impedance changes arise from specific interaction between CRP-Ag and the Ab, at the same time to reveal the selectivity of the binding, contrast experiments were performed. After the immobilization of CRP-Ab and blocking with BSA, the electrode was exposed to various concentrations of an unrelated protein LDL (low-density lipoproteins). LDL is another important index associated with heart disease.[38] Figure 6 shows calibration plots that correspond to the resistance change (ΔR_{et}) with different concentrations of the target analyte (CRP-Ag) and contrast analyte (LDL). The changes of resistance are calculated following the equations:

$$\Delta R_{et} = R_{et(Ab-CRP)} - R_{et(immunosensor)} \quad (2)$$

$$\Delta R_{et} = R_{et(Ab-LDL)} - R_{et(immunosensor)} \quad (3)$$

As can be seen in Figure 6, there is only a slight variation on the impedance with the increase of LDL. Such small changes of the electron-transfer resistance of the nonspecific adsorption are acceptable. This indicated that the observed changes of the electron-transfer resistance with CRP antigen were due to specific antibody−antigen interaction. Without much interference from nonspecific adsorption, the CRP immunosensor has good selectivity.

Precision, Reproducibility, and Stability of the CRP Immunosensor. The reproducibility of the biosensor for CRP was investigated with intra- and interassay precision. The intra-assay precision of the immunosensor was evaluated by assaying one CRP level for three reduplicate measurements, whereas the interassay precision was estimated by measuring one CRP level with three immunosensors prepared independently at the same experimental conditions. The intra- and interassay variation coefficients obtained from 1 ng mL^{-1} CRP were 4.8% and 6.5%, respectively, indicating acceptable precision and fabrication reproducibility. The immunosensor could retain its EIS and CV response after a storage period of 60 days in PBS (10 mM, pH 7.4) at 4 °C, without obvious decline. Evidently, it indicated that the 3DOM gold film electrode prepared by the inverse-opal technique can provide large active surface, which is efficient to retain the bioactivity of antibodies. On the other hand, because of the covalent interaction between MPA-modified gold macroporous structure and primary amine groups in biomolecules, it could also prevent the biomolecules from leaking out. The regeneration of the immunosensor was developed by rinsing with stripping buffer of pH 2.8 Gly−HCl solution to dissociate the Ag−Ab complex. The as-renewed immunosensor could restore 95% of the initial value after five assay runs, showing high reusability and stability. In addition, after five assay cycles, if the immunosensor was further treated with piranha solution to violently peel all the

(38) Havel, R. J.; Kane, J. P. In *The Metabolic Basis of Inherited Disease*, 6th ed.; McGraw-Hill: New York, 1989; Chapter 44A.

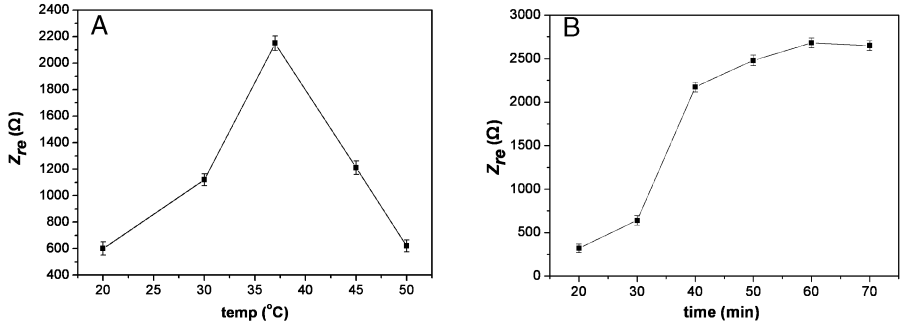

Figure 5. (A) Effect of incubation temperature on Ag−Ab interaction. (B) The effect of Ag−Ab reaction time on the response of EIS.

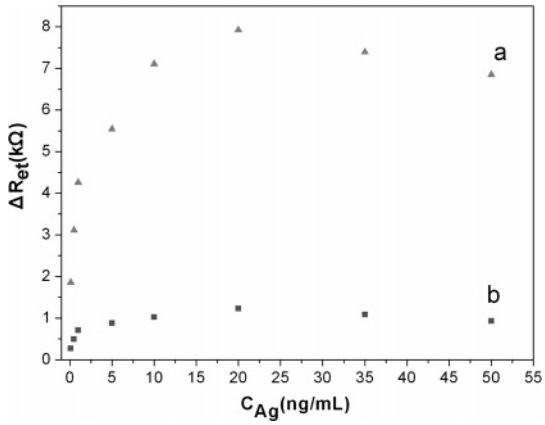

Figure 6. Calibration plots show ΔR_{et} of the different concentrations of (a) CRP antigen and (b) unrelated analyte for the immunosensor.

Table 3. Comparison of Serum CRP Levels Determined Using the Two Methods

sample	proposed method (ng/mL)	turbidimetric or nephelometric homogeneous immunoassay (ng/mL)	relative deviation (%) (ng/mL)
1	1.0	1.1	−9.1
2	5.4	5.2	+3.8
3	17.8	18.7	−4.8

adsorbed MPA and biomolecules from the 3DOM gold substrate surface, complete renewal of the modified electrode could be achieved, with reuse lifetime of more than 20 assay runs.

Application of the Immunosensor in Human CRP Levels. The CRP levels in three serum samples obtained using the proposed immunosensor are shown in Table 3, which compares the results with those obtained from the commercial turbidimetric or nephelometric homogeneous immunoassay technology performed in Nanjing Gulou Hospital for clinical diagnosis. These results indicated the presented method is in good agreement with the traditional clinical method. Thus, this method could satisfy the clinical need for immunoassays of CRP levels.

CONCLUSIONS

A label-free EIS immunosensor was developed upon a 3DOM gold film modified electrode, which was synthesized via the inverted crystal template technique. Due to the large active surface, the special 3DOM gold film electrode possessed superior conductivity, activity, and adsorption capacity. Composed of gold nanoparticles, the film also provided a good microenvironment for the immobilization of proteins while retaining biological activity for the immunosensor. C-reactive protein, a cardiac and inflammation marker, was studied in our impedance immunosensor with both synthetic and real samples using this electrode. This method was stable, versatile, and highly sensitive and could be applied for other immunoassays.

ACKNOWLEDGMENT

The work was supported by the National Natural Science Foundation of China for Distinguished Young Scholars (20325516), the Key Program (20635020), the General Program (20575026, 90606016), and the Creative Research Group (20521503). We also thank the support of the National Basic Research Program of China (2006CB933201). The authors thank Professor Zhen-Lin Wang and Professor Xing-Hua Xia, from the Department of Physics and Department of Chemistry, Nanjing University, respectively, for their kind help. We also thank Professor Wei-Ping Qian from the School of Biological and Medical Engineering, Southeast University, for his warm help.

Received for review October 17, 2007. Accepted January 4, 2008.

AC7021376